

Non-Markovian decoherence of localized nanotube excitons by acoustic phonons

Christophe Galland, Alexander Högele, Hakan E. Türeci, and Ataç Imamoğlu

Institute of Quantum Electronics, ETH Zürich, Wolfgang-Pauli-Strasse 16, CH-8093 Zürich, Switzerland

(Dated: October 22, 2018)

We demonstrate that electron-phonon interaction in quantum dots embedded in one-dimensional systems leads to pronounced, non-Markovian decoherence of optical transitions. The experiments we present focus on the line shape of photoluminescence from low-temperature axially localized carbon nanotube excitons. The independent boson model that we use to model the phonon interactions reproduces with very high accuracy the broad and asymmetric emission lines and the weak red-detuned radial breathing mode replicas observed in the experiments. The intrinsic phonon-induced pure dephasing of the zero-phonon line is two orders of magnitude larger than the lifetime broadening and is a hallmark of the reduced dimensionality of the phonon bath. The non-Markovian nature of this decoherence mechanism may have adverse consequences for applications of one-dimensional systems in quantum information processing.

In single-wall carbon nanotubes (SWNTs), the one-dimensional (1D) nature of electronic states results in an enhancement of Coulomb interactions and has led to the observation of remarkable effects such as Luttinger-liquid states in transport experiments [2]. On the other hand, a common feature of the small diameter semiconducting SWNTs is the unintentional confinement of the electronic or excitonic states along the nanotube axis; this leads to the formation of zero-dimensional (0D) quantum dot (QD)-like states, manifesting themselves through Coulomb blockade in transport experiments [3, 4] or through localized emission [5] and strong anti-bunching in photoluminescence (PL) [6]. Spatial confinement of electrons or excitons in SWNTs is in fact desirable for applications in single photonics or quantum information processing (QIP), which in turn motivates theoretical and experimental investigations of elementary physical properties of optically active QDs in SWNTs.

Electron coupling to Raman-active phonon modes such as radial breathing mode (RBM) and G mode has been an invaluable tool for characterizing SWNTs. Interest in long-wavelength acoustic phonons of SWNTs primarily stems from their potential use as nano-mechanical resonators. A question that is of interest from QIP perspective is the decoherence induced by interactions between QD electrons or excitons and 1D acoustic phonons: while this problem has been addressed theoretically for QD excitons in quasi-1D III-V nanowires in the high temperature limit [7] experimental confirmation of predicted features have not been obtained.

In this letter, we analyze the influence of exciton-phonon interactions on the PL line shape of SWNT QDs. We show that the experimental PL spectra consisting of broad and strongly asymmetric lines can be fit with remarkable accuracy using an analytical solution to the independent boson model, over a dynamical range spanning two orders of magnitude and a temperature range varying from 5K to 35K. In our model, we assume that the lowest bright SWNT excitons, formed out of bound electron-hole pairs from the first band-to-band transition E_{11} [8], are confined to form QD-like states; this assumption is justified since PL has been shown to exhibit strong photon antibunching [6]. The principal result of our work is the demonstration that 1D nature of acoustic phonons and the re-

sulting Ohmic exciton-phonon coupling gives rise to strong pure dephasing of spatially localized optical excitations even as we approach the zero-temperature limit. Even though we study localized SWNT excitons in our experiments, we emphasize that our conclusions are valid for localized transitions in any 1D system. Our findings also suggest that simple PL measurements can be used to determine quantities such as the localization length scale of excitons and the deformation potential coupling strength in carbon nanotubes.

We measured the PL from isolated SWNTs at cryogenic temperatures. Details on the experimental setup and sample preparation are given in [6]. Briefly, we deposited surfactant-embedded CoMoCat SWNTs directly on a functionalized solid-immersion lens (SIL) and used a confocal microscope to detect PL upon excitation with a tunable Ti:Sapphire laser (CW or pulsed mode). The sample is placed in a helium bath cryostat and the temperature is controlled locally through a thermo-resistor. As discussed in [6], spatially localized emission and strong photon anti-bunching indicate that the PL signal originates from unintentionally axially confined excitons, i.e. from SWNT QDs. Figure 1 shows typical experimental PL spectra (open circles) at $T = 4.2$ K that we observed: the line shape is clearly asymmetric with a full-width-half-maximum (FWHM) of 3.5 meV. Time-resolved measurements indicate that the PL decay follows a bi-exponential law with a fastest time constant of 36 psec (Fig. 1 inset) in agreement with previous reports (see [9, 10] and references therein), which implies that the measured linewidth is a factor of 100 larger than the lifetime broadening. This particular nanotube PL exhibited strong photon antibunching with a value for the normalized second-order correlation function $g^{(2)}(0) = 0.1$ [6].

To explain this broad and asymmetric PL line shape we develop a theoretical model where we assume a harmonic confinement potential for excitons along the nanotube axis. For confinement length scales that are long compared to the exciton Bohr radius, QD states are superpositions of free excitonic states with envelope wave functions determined by the 1D harmonic oscillator Hamiltonian. We further assume that the confinement is strong enough to lead to well-separated QD levels, with an energy splitting $\Delta E \gg k_B T$, where k_B is the

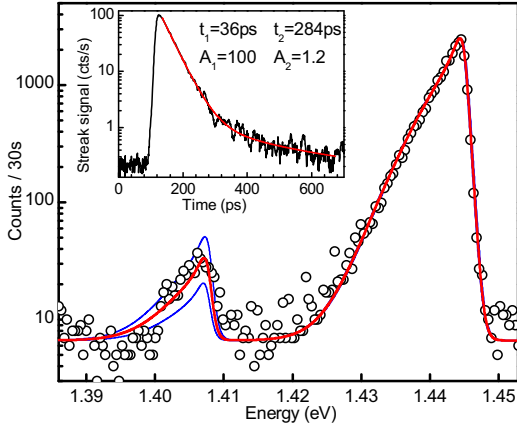


FIG. 1: Photoluminescence of a nanotube quantum dot at $T = 4.2$ K and $P = 300$ nW (open circles) and the calculated spectrum (solid line) plotted on a logarithmic scale. For the theoretical model we used the parameters $D_S = 14$ eV, $D_{RBM} = 1.4$ eV/Å, $\hbar\omega_{RBM} = 37.2$ meV, $\Delta E = 44$ meV and $T_{fit} = 6.3$ K. The upper and lower blue solid lines are calculated spectra with identical parameters but $D_{RBM} = 1.8$ eV/Å and $D_{RBM} = 1.0$ eV/Å, respectively, demonstrating the precision with which the coupling strength can be determined. The inset shows a time-resolved measurement (dark line). The red line is a bi-exponential fit of the PL decay revealing a main fast component with characteristic time $t_1 = 36 \pm 0.2$ ps and weight $A_1 = 100 \pm 0.3$ and a vanishingly weak long tail ($t_2 = 284 \pm 40$ ps, $A_2 = 1.2 \pm 0.2$). From the value of t_1 we expect a lifetime-limited line-width of ~ 0.036 meV, in strong contrast to the measured and calculated width of 3.5 meV.

Boltzmann constant and T the absolute temperature.

To account for the coupling of this QD to the acoustic phonons of the SWNT, we follow the extension of the independent boson model developed in [11]. We assume that the phonon dispersion of the bare SWNT remains unaltered by the confining potential. Since no atomic bonds are formed with the embedding surfactant, we also assume that coupling to phonons of the surrounding material is negligible. Long wavelength acoustic phonons in nanotubes are well described by a continuum elastic model [12, 13] and they couple to electrons through deformation potentials [12, 13, 14]. Because of momentum conservation, only phonon modes with zero angular momentum can couple to excitonic states within a single subband E_{11} ; the potentially relevant modes are therefore stretching, twisting and radial breathing modes. We neglect the coupling to the twisting mode, whose strength is expected to be one order of magnitude smaller than to the stretching mode [12]. The stretching mode corresponds to lattice vibrations with longitudinal displacements of the atoms along the nanotube axis [13]. It has linear dispersion $\omega_s(q) = v_s q$ for small wave-vectors [13] and the strength of its coupling to excitons is characterized by the deformation potential D_S . It would provide the dominant contribution to the broadening of the localized exciton emission, a.k.a. the zero-phonon line (ZPL). Since the RBM has an approximately flat dispersion for small wave-vectors (with an energy $\hbar\omega_{RBM}$), its principal contribution would be the appearance of phonon sidebands in

PL that are separated from the exciton line by $\hbar\omega_{RBM}$.

Following ref [11], we obtain the exciton-phonon matrix elements: $g_j(q) = \mathcal{G}_j(q) \cdot \mathcal{F}^{exc}(q)$ where j stands for S (stretching mode) or RBM . The form factor $\mathcal{F}^{exc}(q) = \int dz |\Psi^{exc}(z)|^2 e^{iq \cdot z}$ provides a cut-off for the coupling in momentum space that is inversely proportional to the spatial extension of the wave function. With our choice of a parabolic potential, we get for the QD ground state a gaussian envelope along z : $\Psi^{exc}(z) = \frac{1}{\pi^{1/4} \sigma^{1/2}} \exp -\frac{z^2}{2\sigma^2}$ where σ is the confinement length. This yields $\mathcal{F}^{exc}(q) = \exp -\frac{q^2 \sigma^2}{4}$ and the energy splitting: $\Delta E = \frac{\hbar^2}{m_{exc}^* \sigma^2}$, where m_{exc}^* is the effective mass of the exciton. The deformation potential couplings are: $\mathcal{G}_S(q) = \frac{D_S \cdot q}{\sqrt{2\rho L \hbar \omega_s(q)}}$ and $\mathcal{G}_{RBM}(q) = \frac{D_{RBM}}{\sqrt{2\rho L \hbar \omega_{RBM}}}$ where L is the length of the nanotube and ρ its linear mass density.

The linear susceptibility $\chi(t)$ ($t \geq 0$) of the QD in response to a δ -shaped laser pulse at $t = 0$ [11, 15] can be decomposed into a temperature-dependent and a temperature-independent contribution $\chi(t) = -ie^{-i\Omega t} \chi_T(t) \cdot \chi_0(t)$ with

$$\chi_T(t) \propto i \exp \sum_q |\gamma_S(q)|^2 [-n_S(q) |e^{-i\omega_S(q)t} - 1|^2] \quad (1)$$

$$\chi_0(t) \propto i \exp \sum_q |\gamma_S(q)|^2 [e^{-i\omega_S(q)t} - 1] \quad (2)$$

where $\gamma_j(q) = \frac{g_j(q)}{\omega_j(q)}$, and $n_j(q) = (e^{\hbar\omega_j(q)/k_B T} - 1)^{-1}$ is the phonon occupation number. The polaron-shifted transition energy is $\bar{\Omega} = \Omega - \sum_{j,q} |\gamma_j(q)|^2 \omega_j(q)$, where $\hbar\Omega$ is the bare energy of the QD-state. Performing the Fourier transform of $\chi(t)$ and taking its imaginary part gives the absorption spectrum of the QD. The PL-emission line shape that we measure experimentally is obtained by taking the mirror image of the absorption profile with respect to the ZPL [16].

The solid curve in Fig. 1 shows that this simple theoretical model describes the experimental observation remarkably well. To obtain this fit, we use SWNT parameters that were reported earlier; in particular, we take $\rho = 1.67 \cdot 10^{-15}$ kg/m, $v_s = 19.9$ Km/s [12] and $m_{exc}^* \simeq 0.2 \cdot m_e$ [17]. An electron-phonon deformation potential for the stretching mode [12, 13] of strength $D_S = 14$ eV has been extracted from data on low-field mobilities in semiconducting SWNTs [14] [26]. Our procedure, applied to 10 different SWNT spectra, involves varying the values of D_S and the confinement to obtain the best fit to the data. The range of D_S values we thereby obtained varied from 12 to 14 eV. The other fitting parameter is the confinement potential along the SWNT axis which determines the cut-off in momentum space, or equivalently the level spacing ΔE . We found values for ΔE between 20 and 44 meV, consistent with our assumption $\Delta E \gg k_B T \approx 2.8$ meV (at 35 K) and corresponding to an extension of the wave function envelope on the order of ~ 10 nm. Since this confinement length-scale is bigger than the Bohr radius [8, 18], our assumption of exciton center-of-mass confinement is also justified.

The PL spectrum from Fig. 1 is plotted on a logarithmic vertical scale to show the quality of the fit over two decades of counts and to emphasize the presence of a red-detuned replica

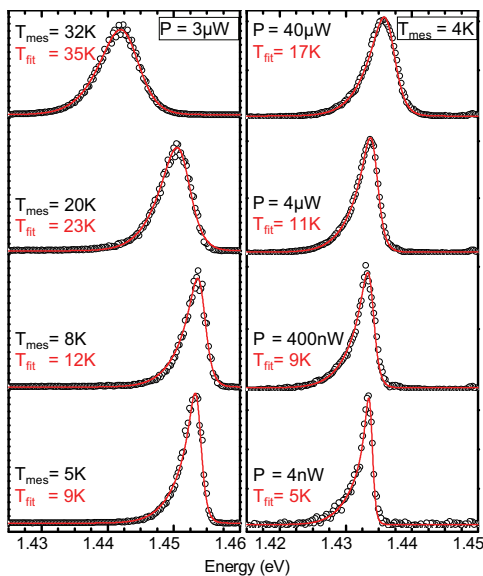


FIG. 2: Left panel: Experimental (open circles) and calculated (red solid lines) PL spectra for the same SWNT at different temperatures T_{mes} (the vertical scale is arbitrary). The excitation power was kept constant at $P = 3\mu W$. The effective temperature used in the simulation is given by T_{fit} , the other parameters are $D_S = 12.7$ eV and $\Delta E = 22$ meV. Right panel: Emission from another nanotube at constant sample temperature $T = 4.2$ K. The changes induced by increasing the laser intensity from 4 nW to 40 μW are very well reproduced by increasing the temperature T_{fit} in the model. The parameters for this SWNT are $D_S = 13$ eV and $\Delta E = 20$ meV.

that is exactly reproduced by the model. The RBM deformation potential for excitons are well documented [19, 20, 21] and expected to lie between 1 and 2 eV/Å. Here we obtained the best fit for $D_{RBM} = 1.4 \pm 0.2$ eV/Å and a RBM energy of 37.2 meV corresponding to a SWNT diameter of about 0.7 nm, in good agreement with CoMoCat SWNTs emitting at this wavelength. The linear power dependence of the red-detuned replica for very low excitation intensities (not shown) is consistent with that of a phonon sideband and excludes an explanation based on biexciton emission.

Figure 2 shows the experimental PL lines (open circles) for two different SWNTs. In the left panel, the temperature is increased by flowing current in the thermo-resistor. The very asymmetric lines at the lowest temperatures and the evolution to broader symmetric lines with increasing temperature is a general feature common to virtually all of the 30+ SWNTs that we measured. The computed spectra (solid red lines) reproduce both qualitatively and quantitatively this behavior when the coupling to the stretching mode only is taken into account. Only the considerable shifts in the transition energies are not reproduced by the model; arbitrary offsets were therefore introduced for each spectrum. This unexpected sensitivity on minor environmental changes is another evidence for localized emitting states [6]. In contrast, the transition energy of a delocalized exciton is not expected to shift so dramatically with temperature [22].

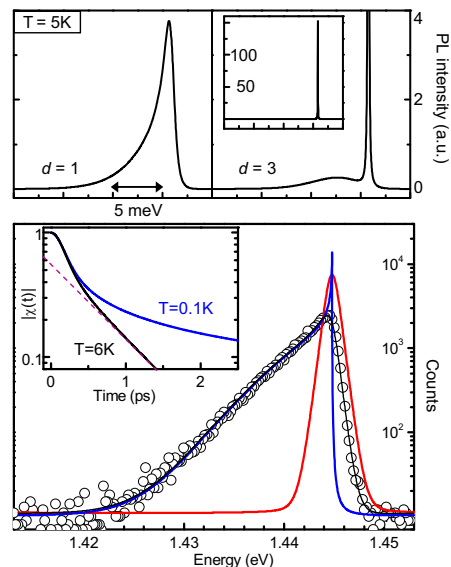


FIG. 3: Upper panel: Calculated emission line-shapes at $T = 5$ K for a QD coupled to a phonon bath of dimension $d = 1$ (left) and $d = 3$ (right) are shown. The coupling to a single acoustic phonon branch with linear dispersion ($v_s = 19.9$ Km/s) is considered. To extend the model to higher dimension, we assume an isotropic coupling of the QD to LA phonons described by the same deformation potential. A lifetime broadening corresponding to $t_1 = 36$ ps is introduced. Lower panel: For illustration, fit of the spectrum shown in Fig. 1 (open circles) with only the temperature dependent (Eq. 1, red line) and the temperature-independent (Eq. 2, blue line) contributions. Each curve is scaled to span the same total area. The inset shows the susceptibility ($T = 6$ K) used to fit the data (black curve), where a deviation from an exponential decay is visible for $t \leq 1$ ps. The blue curve of the inset shows the same function at $T = 0.1$ K where the non-Markovian nature of dephasing becomes clearer.

The right panel in Fig. 2 (different SWNT) shows that the effect of increasing the excitation power can be reproduced by only increasing the temperature of the phonon bath in the model and keeping all the other parameters fixed. From this, one can conclude that the laser excitation led to a very local heating of the SWNT that was not directly measured by our thermo-resistor placed about 1 mm away from the nanotubes.

We emphasize that the unusually broad lines observed in SWNT PL can be accurately and quantitatively explained by solely taking into account interaction with long wavelength 1D acoustic phonons. The resulting ohmic coupling [23] gives rise to linewidths that are two orders of magnitude larger than the ones expected from lifetime broadening. To highlight this feature, we have plotted in Fig. 3 a comparison of the theoretical PL line shape for a QD interacting with 1D and 3D phonon reservoirs. Coupling to 2D or 3D acoustic phonons yields a superohmic spectral function [23], for which the independent boson model predicts a (lifetime-broadened) ZPL accompanied by phonon sidebands (Fig. 3, upper right). This is in strong contrast to our observations from SWNTs. [27]

The enhanced pure dephasing of QD transitions in 1D structures was analyzed theoretically in Ref. [7] where the fi-

nite width was attributed to the high temperature (Markovian) limit. This part is due to the temperature-dependent contribution $\chi_T(t)$ in Eq.(1) and vanishes linearly as $T \rightarrow 0$. It provides a symmetric contribution to the line shape (as illustrated in Fig. 3, lower panel, red curve). In contrast, the highly asymmetric character of the observed line shapes at low temperatures is largely due to the temperature-independent part of the susceptibility, $\chi_0(t)$, in Eq.(2). For comparison, we plot these two contributions separately, although they appear in the line shape as a convolution. The temperature-dependent term is responsible for the presence of a high-energy tail at non-zero temperature, while the broad low-energy tail we measure constitutes a direct signature of the temperature-independent pure dephasing. Furthermore, we find that the characteristic energy of the latter quasi-exponential tail is directly proportional to the width of the form factor in q -space. This dependence is to be expected since the inverse localization length scale determines the highest phonon energies to which the QD is effectively coupled. A stronger confinement therefore leads to a faster dephasing, even at arbitrarily low temperatures.

In Fig. 3 (lower panel) the inset shows the time dependence of the calculated linear susceptibility $\chi(t)$ used to fit the experimental spectrum: the deviation from an exponential decay that is apparent for $t \leq 1$ psec is a hallmark of non-Markovian decoherence [24]. Our calculations indicate that this initial (Gaussian) decay crosses over to a power-law decay and finally to an exponential decay at long times. The regime where power-law decay is dominant expands as temperature is decreased; further reduction of the temperature to 0.1K leads to the appearance of power-law decay of the susceptibility extending to 15 psec (blue curve). Observation of such a strong deviation from Markovian dynamics should be within reach.

To conclude, we have used an extension of the independent boson model to reproduce with remarkable quantitative accuracy the asymmetric and broad lines that we measured on isolated SWNTs. The model also reveals the changes in the shape and width with temperature. In strong contrast to 3D systems, the reduced dimensionality of the phonon bath in SWNTs leads to ohmic coupling of confined excitons to stretching mode phonons: in this limit, the ZPL is replaced by a power-law singularity. This conclusion remains valid at arbitrarily low temperatures, where the induced pure dephasing becomes manifestly non-Markovian, and would apply to QDs defined in any one-dimensional system. These intrinsic

effects are of fundamental interest in view of applications in quantum information processing, where non-Markovian nature of decoherence may substantially alter the attainable accuracy thresholds [25].

The Authors acknowledge enlightening discussions with Ignacio Wilson-Rae. This work was supported by a grant from the Swiss National Science Foundation (SNSF).

-
- [1] M. S. Dresselhaus, G. Dresselhaus, Ph. Avouris, *Carbon Nanotubes* (Springer-Verlag, Berlin, 2001).
 - [2] H. Ishii *et al.*, *Nature* **426**, 540-544 (2003).
 - [3] B. Gao *et al.*, *Phys. Rev. B* **74**, 085410 (2006).
 - [4] P. L. McEuen *et al.*, *Phys. Rev. Lett.* **83**, 5098 (1999).
 - [5] A. Hartschuh *et al.*, *Nano Lett.* **5**, 2310-2313 (2005).
 - [6] A. Högele *et al.*, *Phys. Rev. Lett.* **100**, 217401 (2008).
 - [7] G. Lindwall *et al.*, *Phys. Rev. Lett.* **99**, 087401 (2007).
 - [8] R. B. Capaz *et al.*, *Phys. Rev. B* **74**, 121401 (2006).
 - [9] A. Hagen *et al.*, *Phys. Rev. Lett.* **95**, 197401 (2005).
 - [10] H. Hirori *et al.*, *Phys. Rev. Lett.* **97**, 257401 (2006).
 - [11] B. Krummheuer, V. M. Axt, T. Kuhn, *Phys. Rev. B* **65**, 195313 (2002).
 - [12] H. Suzuura, T. Ando, *Phys. Rev. B* **65**, 235412 (2002).
 - [13] G. Pennington, N. Goldsman, *Phys. Rev. B* **71**, 205318 (2005).
 - [14] G. Pennington *et al.*, *Appl. Phys. Lett.* **90**, 062110 (2007).
 - [15] A. Vagov, V. M. Axt, T. Kuhn, *Phys. Rev. B* **66**, 165312 (2002).
 - [16] Mahan, *Many-particle Physics, Third edition*, p 234-235 (Plenum, New York, 1990).
 - [17] T. G. Pedersen, *Carbon* **42**, 1007-1010 (2004).
 - [18] J. Maultzsch *et al.*, *Phys. Rev. B* **72**, 241402 (2005).
 - [19] Y. Yin *et al.*, *Phys. Rev. Lett.* **98**, 037404 (2007).
 - [20] A. P. Shreve *et al.*, *Phys. Rev. Lett.* **98**, 037405 (2007).
 - [21] J. Jiang *et al.*, *Phys. Rev. B* **72**, 235408 (2005).
 - [22] D. Karaiskaj *et al.*, *Phys. Rev. Lett.* **96**, 106805 (2006).
 - [23] I. Wilson-Rae and A. Imamoglu, *Phys. Rev. B* **65**, 235311 (2002).
 - [24] D. Divincenzo, D. Loss, *Phys. Rev. B* **71**, 035318 (2005).
 - [25] B. M. Terhal, G. Burkard, *Phys. Rev. A* **71**, 012336 (2005).
 - [26] We note that this is a measure of the electron-phonon coupling, whereas the relevant value in our case is the difference between the electron and hole deformation potentials, which has never been measured so far.
 - [27] We note, however, that the observed line shapes could also be reproduced using a subohmic spectral function that would be relevant for confined excitons coupled to 1D bending modes. The presence of such a coupling on the other hand, requires the breaking of the circumferential symmetry of the confined excitonic wave function.